1 Model evaluation for Technology E

1.1 Device information

The provided device is a 12GHz transistor fabricated in a BiCMOS foundry process. The transistor size is $0.6*4.8\mu m^2$.

- The provided data consists of
  - de-embedded S-parameters as a function of bias and frequency for V_{BC} = const(various values); T = 21.4C is given as information in respective file headers.
  - DC bias data, measured on the same device and for same V_{BC}, but at a different temperature T=24.2.

1.2 Parameter extraction

The de-embedded S-parameter data (incl. bias information) were converted to y-parameters. In particular, data with constant f = 1GHz were derived for the determination of f_T and an overall comparison of y-parameters over bias. For parameter extraction, only the consistent data set from S-parameter measurements (“AC” data) were employed to avoid having to deal with different temperatures during extraction and fine-tuning (changing temperature would increase effort, time and error probability during extraction). However, the same parameters were then also used, with some of them adjusted according to the additional information available at lower current densities, to compare the DC data (obtained from pure DC measurements) at the corresponding temperature.

Junction capacitance data (containing depletion and isolation components) were obtained from “cold” measurements. Figs. 1.2/1 to 1.2/3 show the comparison between measured data (symbols) and model (lines). Note the extended scale by suppressing the y-axis origin.

Substrate transistor action seemed to be negligible, and the corresponding parameters were omitted.

Below, first the results obtained for the AC data set are shown, followed by the results for the DC data set (and additional comments). In many cases the data are plotted vs. the (log of) collector current density I_C/A_E rather than vs. V_{BE}. The latter is of little interest and use for circuit design, and does not provide circuit design related information on the bias point. Note, that $V_{BE} \sim \log(I_C)$ for low current densities.

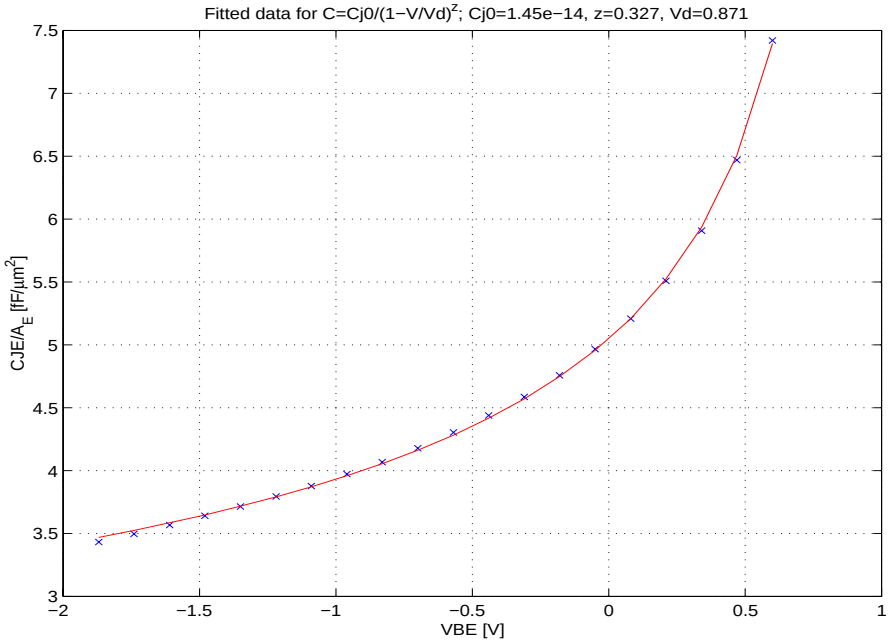

Fig. 1.2/1: Base-emitter capacitance vs. V_{BE}: measurement (symbols), HICUM (line).

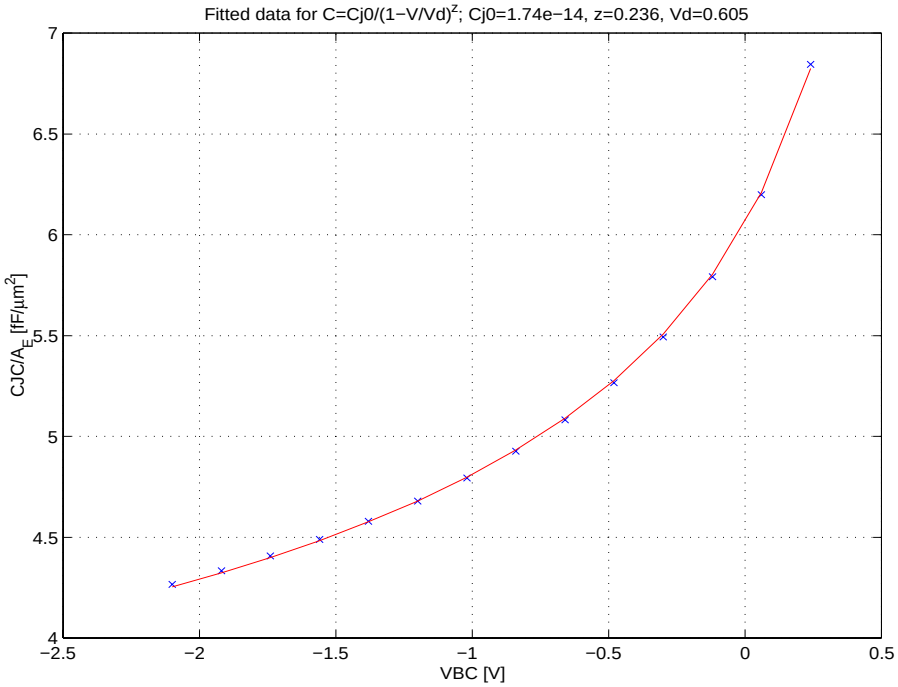

Fig. 1.2/2: Base-collector capacitance vs. V_{BC}: measurement (symbols), HICUM (line).

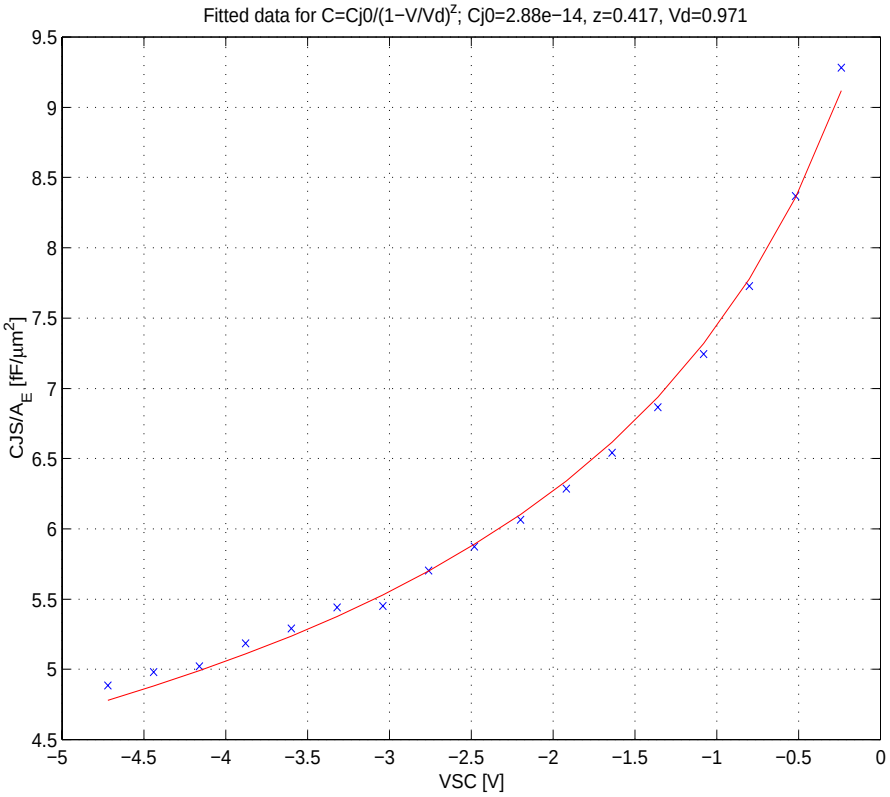

Fig. 1.2/3: Collector-substrate capacitance vs. V_{SC}: measurement (symbols), HICUM (line).

1.3 Results for the AC measurement data (T=21.4C)

Figures 1.3/1 to 1.3/3 contain a comparison of standard characteristics between model (solid lines) and measurements (symbols) within the interesting and available collector current density range. In all cases, fairly good agreement has been obtained at least up to the current density where f_T peaks. At very high current densities, slight deviations can be observed for the base current. Such deviations can be caused by uncertainties in, e.g., series resistances, self-heating and associated temperature coefficients.

Fig. 1.3/5 shows the y-parameters as a function of collector current density at f = 1GHz and constant V_{BC} values. Excellent agreement is obtained for almost all curves.

Figures 1.3/6 to 1.3/9 contain comparisons of frequency dependent y-parameters for selected bias points. In the first two figures, a set of curves was picked for V_{BC} = 0.5V, which is an extreme case, especially at high current densities: Fig. 1.3/7 shows fairly good results for a current density, that is close to f_T peak. In the last two figures, the curves were selected for the highest available (reverse) voltage V_{BC}=-3V in order to demonstrate the capability of HICUM to cover a larger bias range without loss of accuracy. For both voltages, the agreement at the lower current densities (Figs. 1.3/6 and 1.3/8) is also quite good.

At low frequencies, the measurement uncertainty does not always allow a clear conclusion. For the transistor provided, a simple substrate resistance HICUM seems to be sufficient for accurate modeling of the substrate coupling in y_{22}.

In summary, all characteristics show acceptable agreement even beyond peak f_T.

The combination of model parameter values found during fitting (cf. Fig. 1.3/10) describes the characteristics in the operating regions of interest quite well, but can be improved in some regions if additional measured data and proper test structures would be available to separate various physical as well as geometry related effects.

Note that (a) f_T peaks - depending on V_{BC} - between J_C values of 0.2 and 0.5 mA/μm^2; (b) operation beyond peak f_T is of interest only for circuits switching at high-speed, in which the dynamic base current can become much larger than the DC base current, making accurate DC base current modeling irrelevant compared to accurate modeling of charges which is reflected by f_T and in some cases also by, e.g., f_{max}.

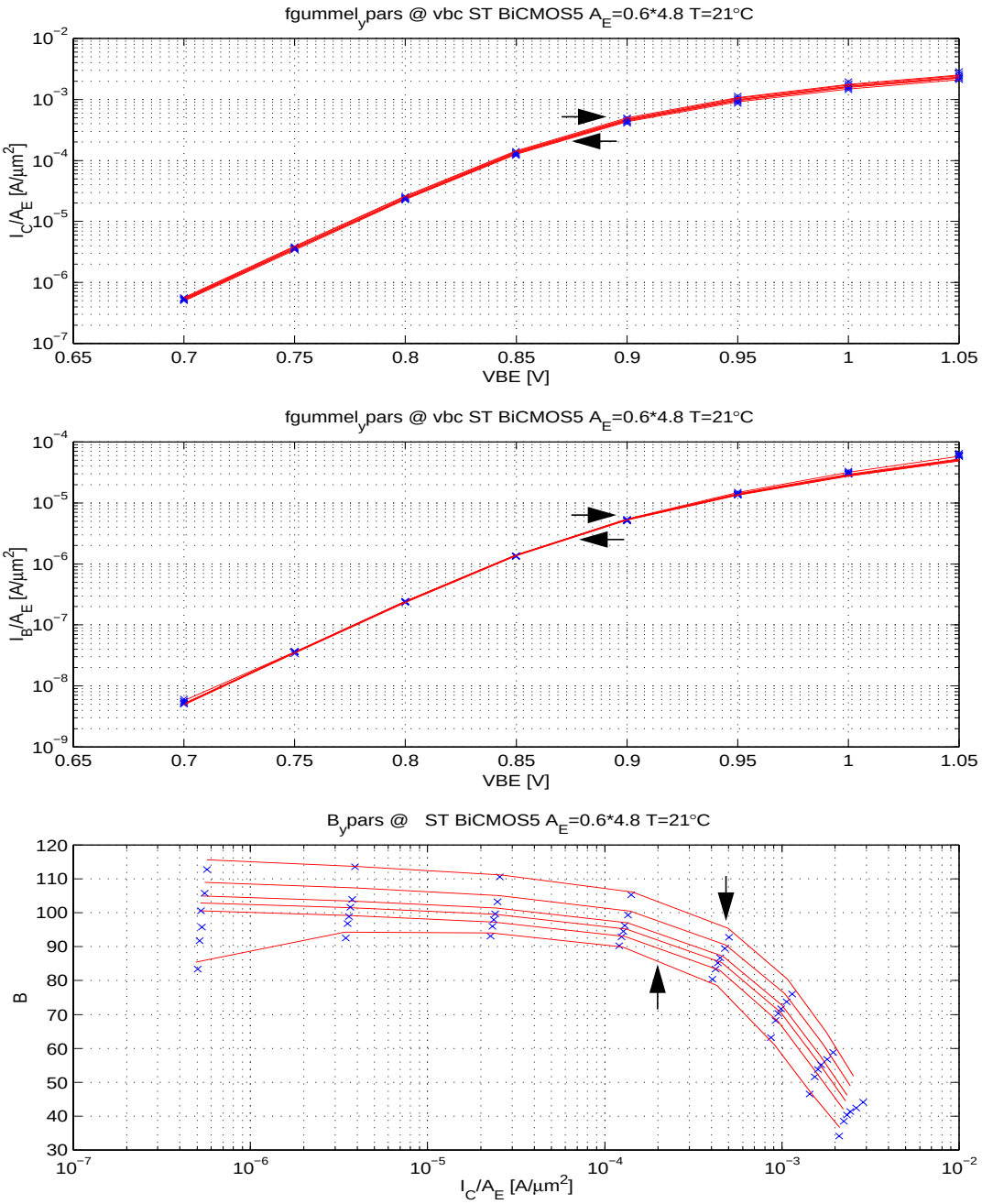

Fig. 1.3/1: Collector current density vs. V_{BE} ,Base current density vs. VBE,
Current gain vs. collector current density
for V_{BC}/V = 0.5, 0, -0.5, -1, -2, -3; T=21.4C. Data source: AC measurements.
The arrows indicate peak f_T for the lowest and highest V_{BC} value

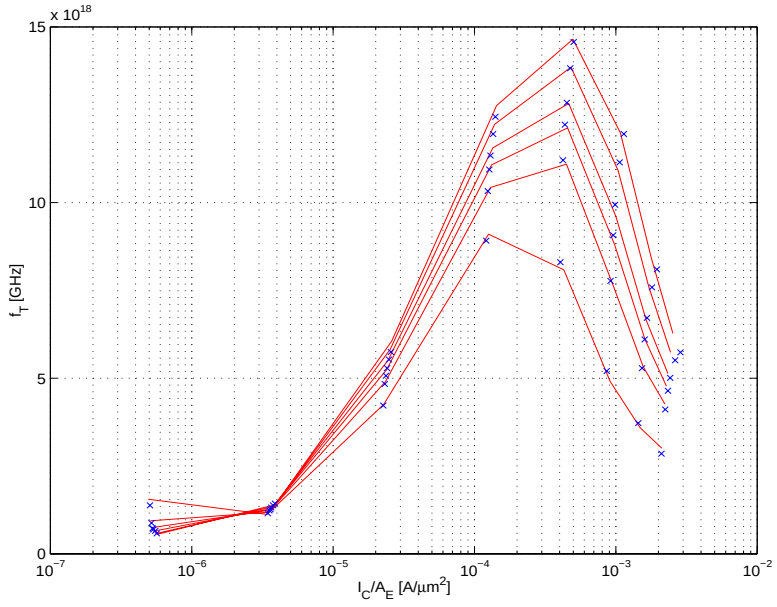

Fig. 1.3/2: Extracted transit frequency vs. collector current density
for V_{BC}/V = 0.5, 0, -0.5, -1, -2, -3; T=21.4;
model bias points according to the provided measurements

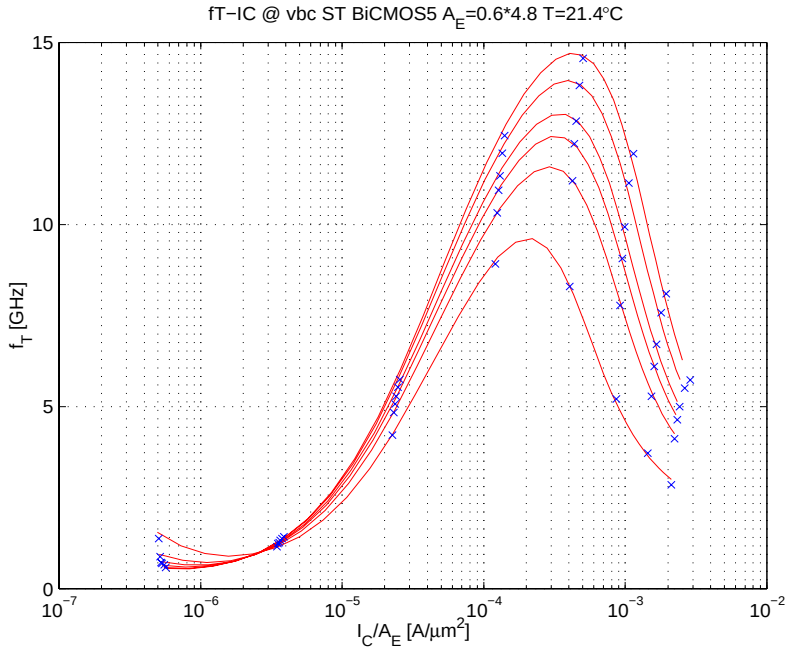

Fig. 1.3/3: Simulation for f_T with more model bias points for smoothing

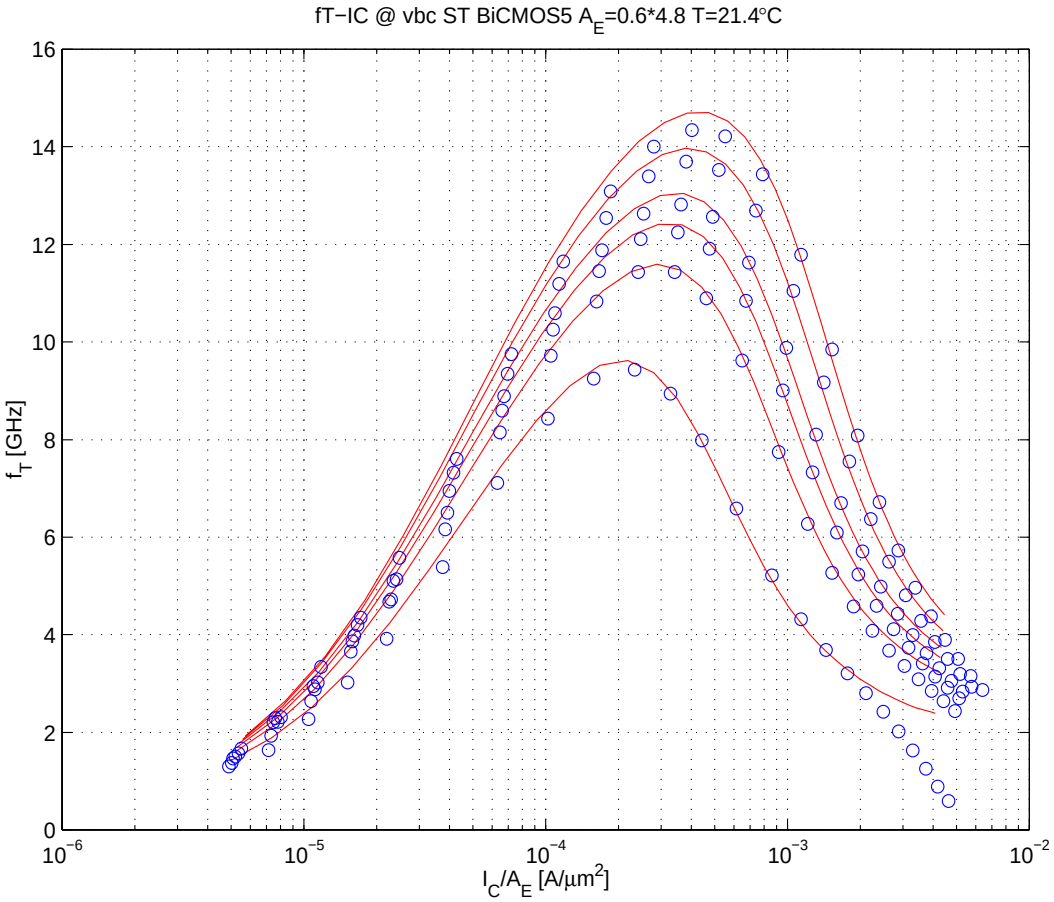

Fig. 1.3/4: Transit frequency vs. collector current density for V_{BC}/V = 0.5, 0, -0.5, -1, -2, -3; T=21.4;
measured f_T determined from y-parameters; simulation with AC model parameters.

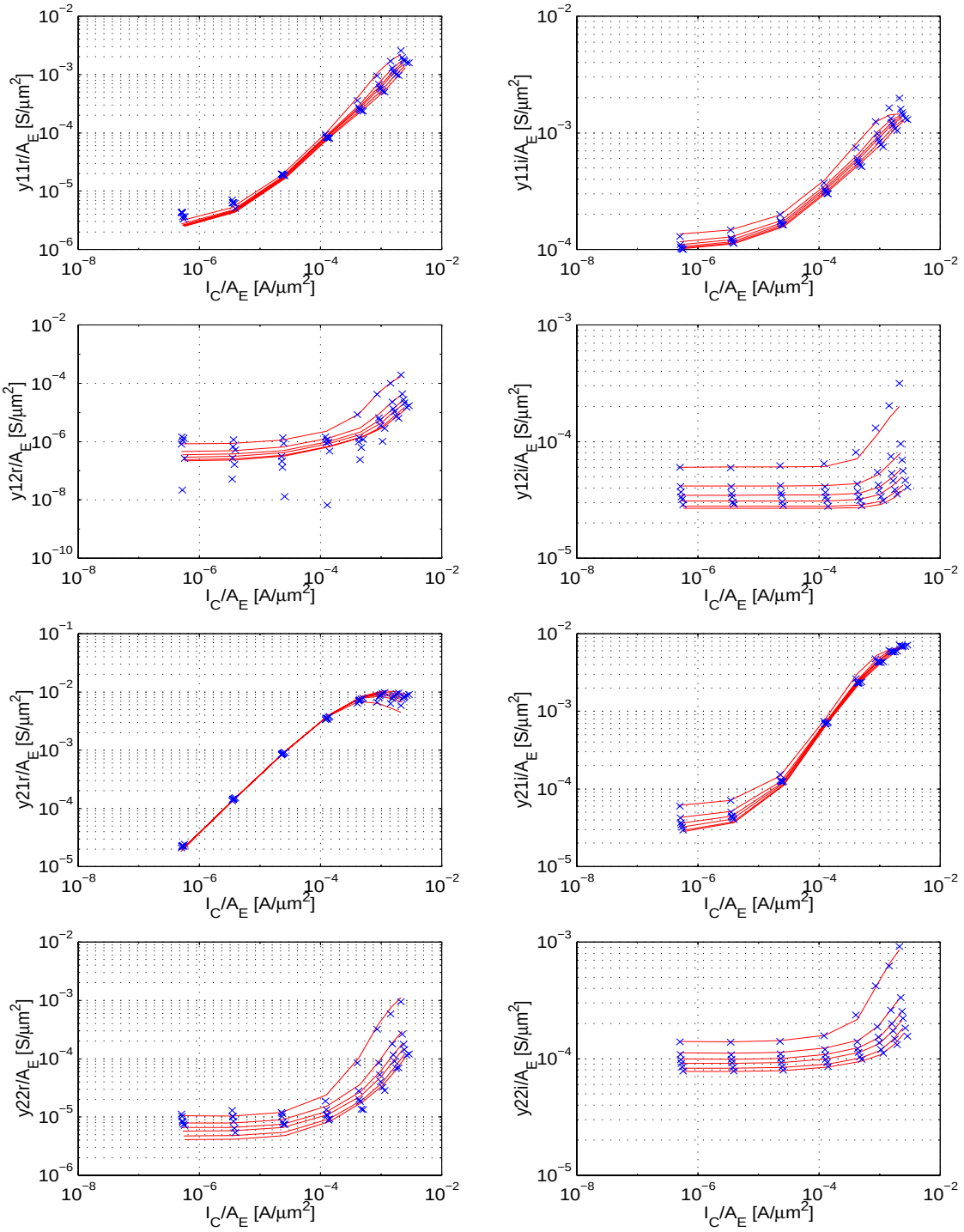

Fig. 1.3/5:Y-parameters vs. collector current density at f=1GHz; V_{BC}/V = 0.5, 0, -1, -3; T=21.4C.

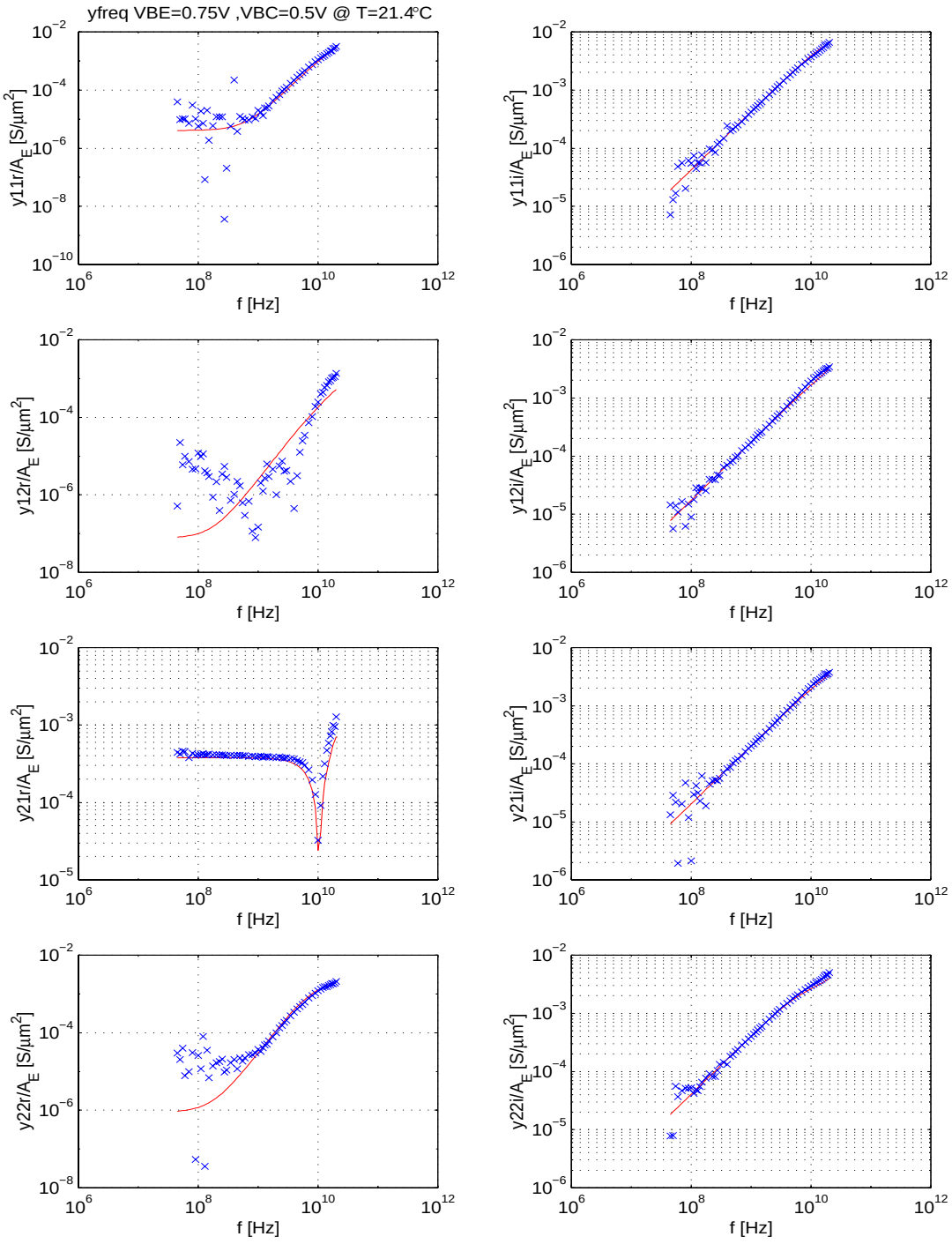

Fig. 1.3/6: Frequency dependent y-parameters at V_{BC} = 0.5V and I_C/A_E below peak f_T.

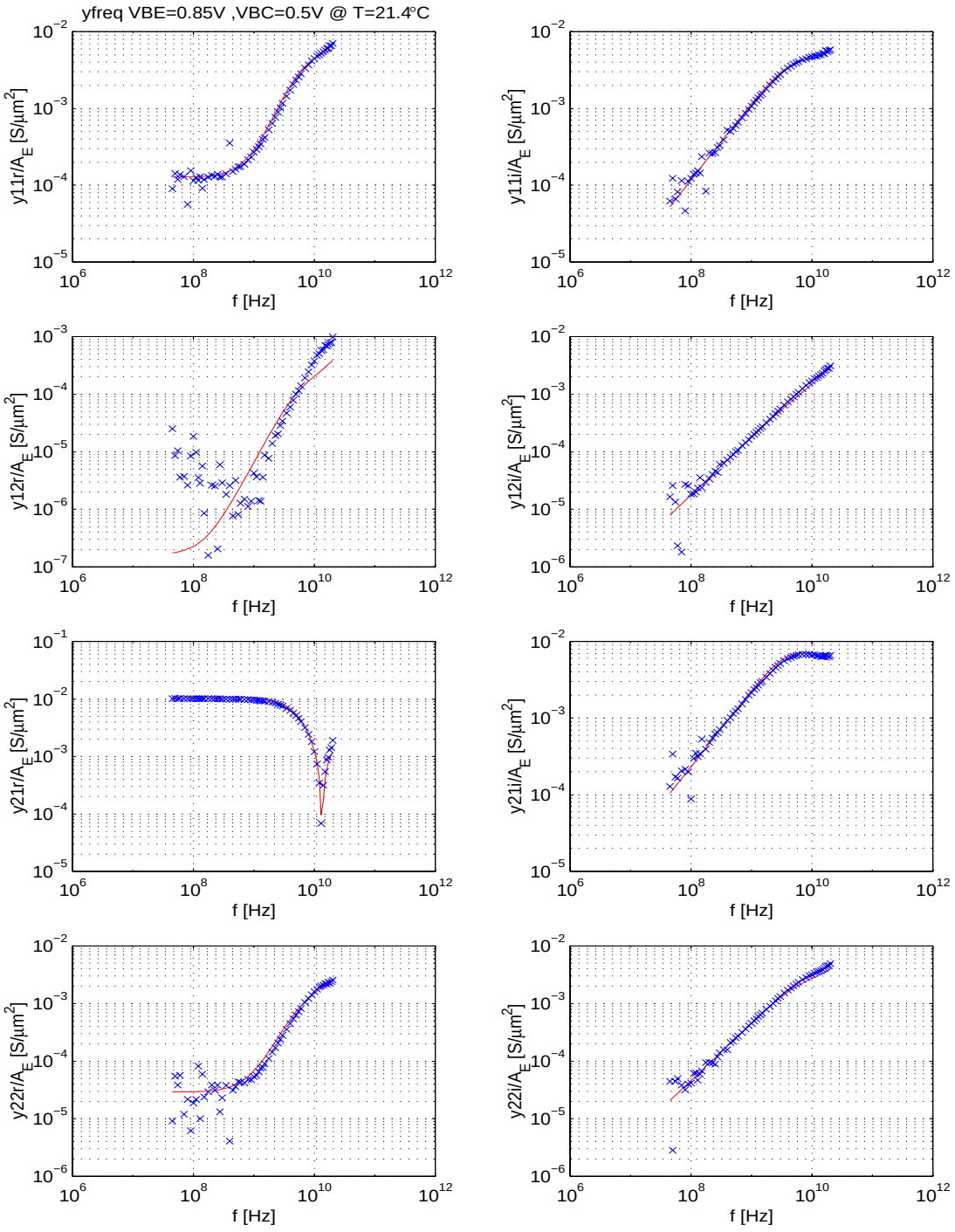

Fig. 1.3/7: Frequency dependent y-parameters at V_{BC} = 0.5V and I_C/A_E close to peak f_T.

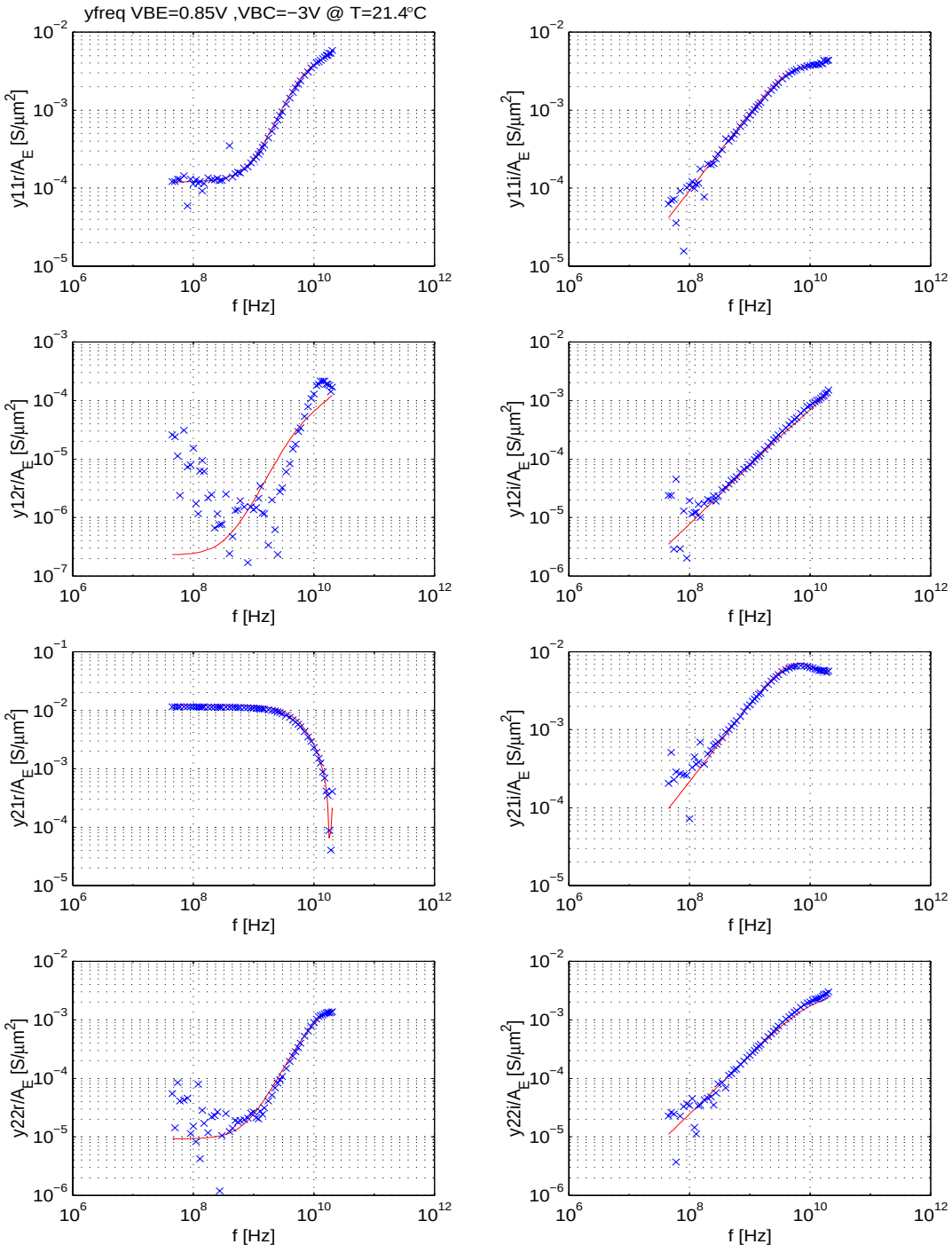

Fig. 1.3/8: Frequency dependent y-parameters at V_{BC} = -3V and I_C/A_E below peak f_T.

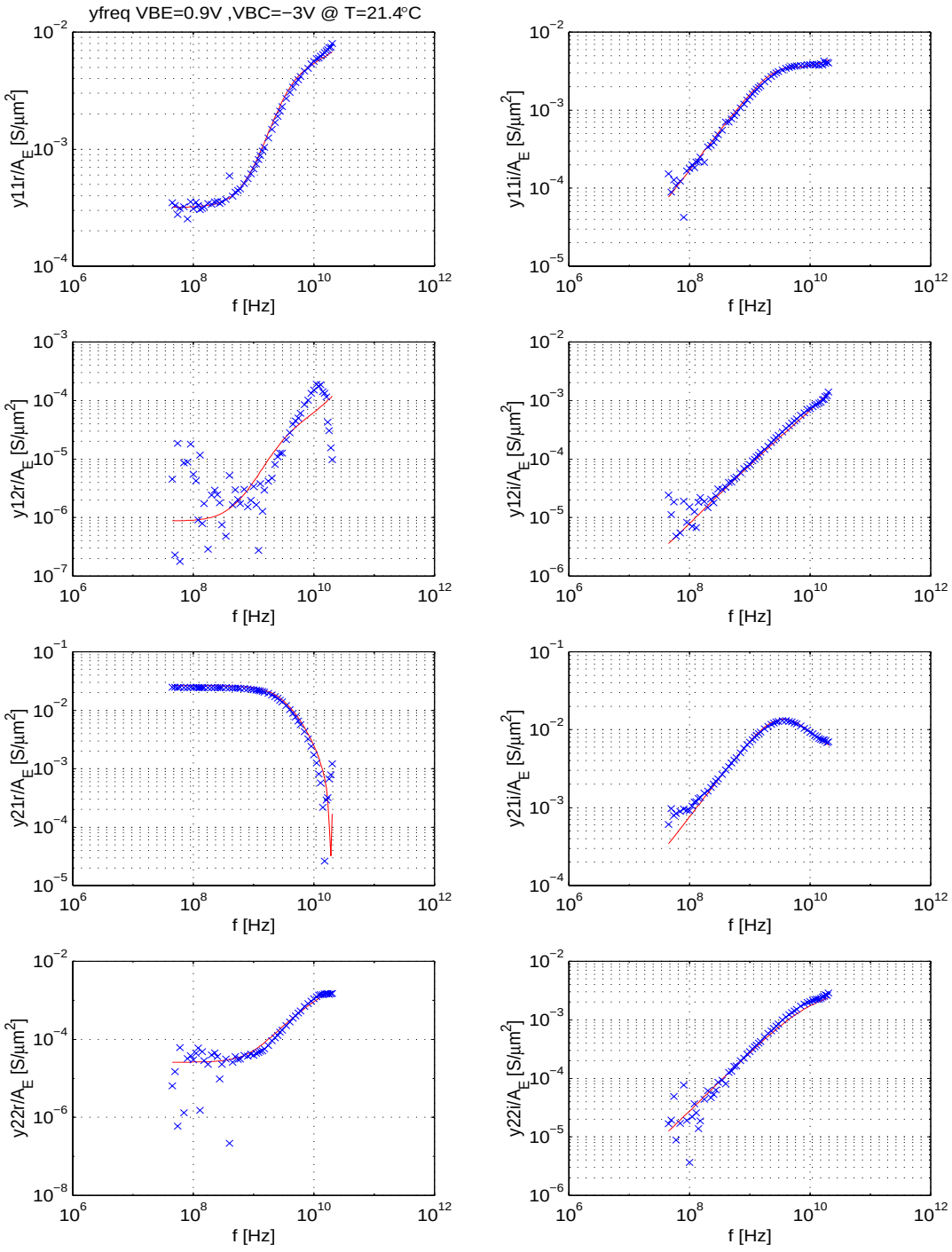

Fig. 1.3/9: Frequency dependent y-parameters at V_{BC} = -3V and I_C/A_E at peak f_T.

```
'*'  HICUM / LEVEL2  AC-Satz
'MODQ' 'Tref' 1
 &HICUM2 c10=4.78E-32     qp0=2.25E-14     ich=5.20E-03     hfc= 0.20
       hfe= 1.00       hjci= 0.77       hjei= 1.00       alit=0.450
       cjei0=8.88E-15   vdei=0.960       zei=0.595        aljei= 2.20
       cjci0=2.12E-15   vdci=0.780       zci=0.474        vptci=1.05E+01
       t0=1.02E-11      dt0h=-1.170E-12  tbvl=5.300E-13   tef0=2.55E-13
       gtfe=  1.00      thcs=5.9E-11     alhc= 8.143      fthc= 0.800
       alqf=0.225
       rci0=4.5E+01     vlim= 0.387      vpt=  4.19       vces= 0.100
       tr=0.00E+00
       ibeis=1.89E-20   mbei=1.0080      ireis=7E-17   mrei=2.0000
       ibcis=1.00E-30   mbci=1.0240
       favl=3.000       qavl=4E-14
       rbi0= 125.50     fdqr0=0.200      fgeo=0.7570      fqi=1.0000
       fcrbi=0.20
       latb=3.470E+00   latl=0.434
       cjep0=7.95E-15   vdep=0.980       zep=0.437        aljep= 2.30
       ibeps=1.00E-30   mbep=1.0110      ireps=1.00E-30   mrep=2.0000
       ibets=0.00E+00   abet=  0.00
       cjcx0=1.42E-14   vdcx=0.835       zcx=0.452        vptcx=2.30E+00
       ccox=2.78E-15    fbc=0.128
       ibcxs=13E-18     mbcx=1.045
       ceox=1.13E-15    rbx=  76.19      re= 15.500       rcx=  16.75
       itss=1.00E-30    msf=1.000        tsf=0.00E+00
       iscs=1.00E-30    msc=1.000
       cjs0=4.01E-14    vds=0.650        zs=0.282         vpts=1.00E+03
       rsu=    500.0    csu=0.00E+00
       kf=0.00E+00      af=1.00E+00
       vgb= 1.160       alb= 1.60E-03    alt0= 0.00E+00   kt0= 0.00E+00
       zetaci=  1.600   alvs=1.00E-03    alces=4.00E-04   zetarbi=  0.830
       zetarbx=  0.180  zetarcx=  0.190  zetare= -0.800
       alfav=8.25E-05   alqav=1.96E-04
       rth= 400.00      cth=0.00E+00  &end
```

Fig. 1.3/10: Set of model parameters for the AC measurement based comparison (DEVICE).

1.4 Comparisons to measured DC data (T= 24.2C)

Figure 1.4/1 contains a comparison of DC characteristics between model (solid lines) and measurements (symbols). These DC data cover a larger bias range towards *very low* current densities but contain, in contrast to the data from AC measurements, only a subset of V_{BC} values. For the comparison, most model parameters (cf. Fig. 1.4/8) were left unchanged from the previous ("AC") values, except the ones modeling the various base current components at low current densities and the avalanche current, for which insufficient data was available from "AC" measurements. The current gain drops at much lower current densities compared to the data from AC measurements, requiring to re-adjust the corresponding base current parameters. In general, similar agreement is obtained for the same characteristics that were already compared for the data set from AC measurements. Also, good agreement is obtained for the bias region at very low current densities.

In addition to the usual DC characteristics, several low-frequency derivatives, i.e. (normalized) conductances, are shown.

- Fig. 1.4/2a, the normalized transconductance

$$\frac{g_m}{I_C} = \frac{1}{I_C}\left.\frac{dI_C}{dV_{BE}}\right|_{V_{BC}} . \tag{1.4.0-1}$$

  The observed deviations might be due to insufficient information on the partitioning of internal and peripheral base emitter capacitance which cannot be obtained from a single device.

- Fig. 1.4/2b, the normalized input conductance

$$\frac{g_{BE}}{I_B} = \frac{1}{I_B}\left.\frac{dI_B}{dV_{BE}}\right|_{V_{BC}} \tag{1.4.0-2}$$

- The deviations at very high current densities can be due to the unknown partitioning of various effects (as already discussed before) and would need further investigation. However, the importance of the above characteristic for circuit design is unclear.
- In Fig. 1.4/3b, the output conductance:

$$g_o = \left.\frac{dI_C}{dV_{CE}}\right|_{I_B} . \tag{1.4.0-3}$$

  The agreement is fairly good over the entire bias range. Deviations are believed mainly to be due to (a) insufficient knowledge about the voltage dependence of the internal BC junction capacitance (cannot be extracted from a single device) and other relevant parameters, and (b) the weak avalanche model that does not take into account the breakdown mechanism at high current densities (which occurs close to the buried layer).

All derivatives were obtained by numerical differentiation.

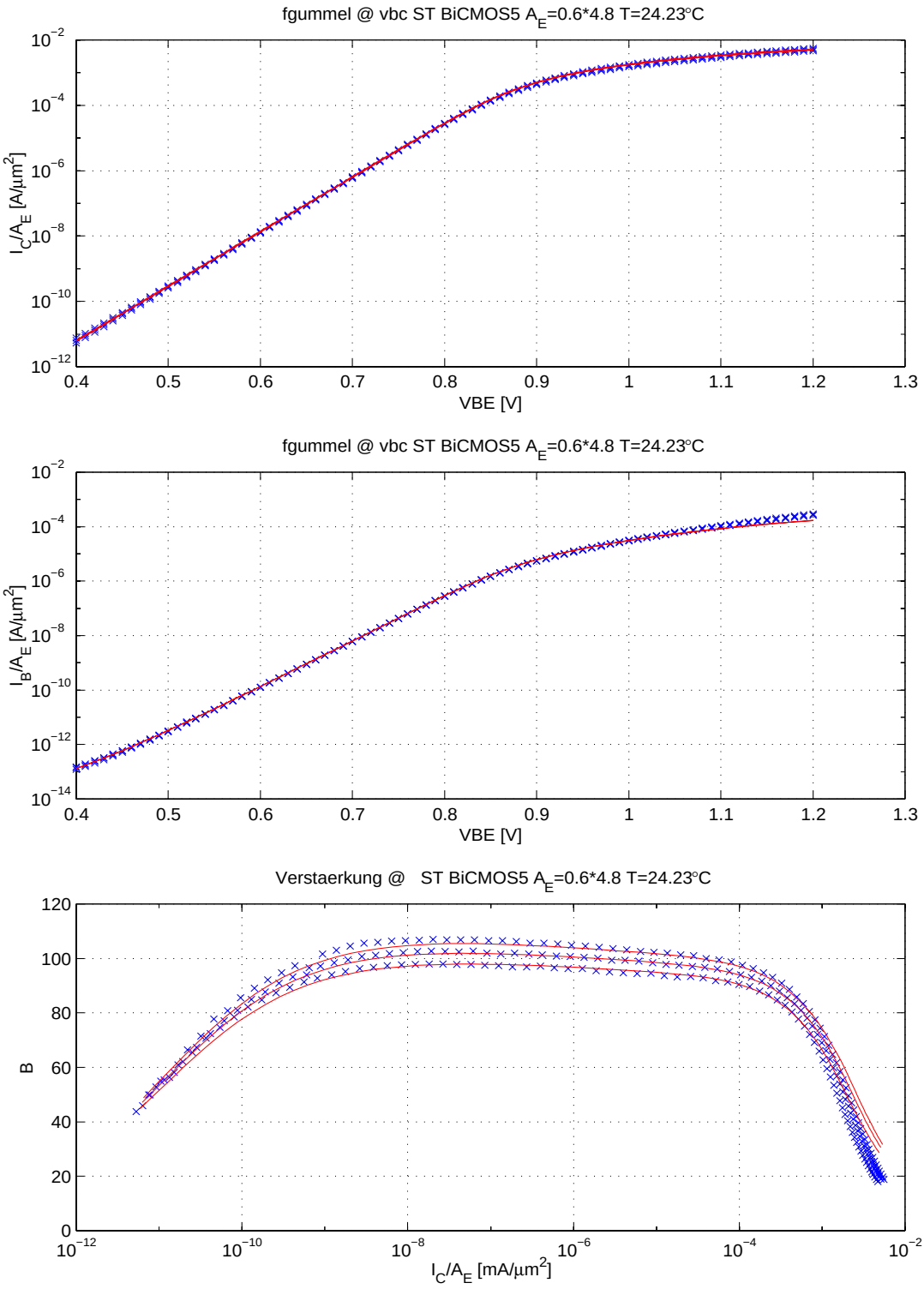

Fig. 1.4/1: Forward gummel characteristics and DC current gain for V_{BC}/V = 0, -1, -2; T=24.2C. Data source: DC measurements.

a)

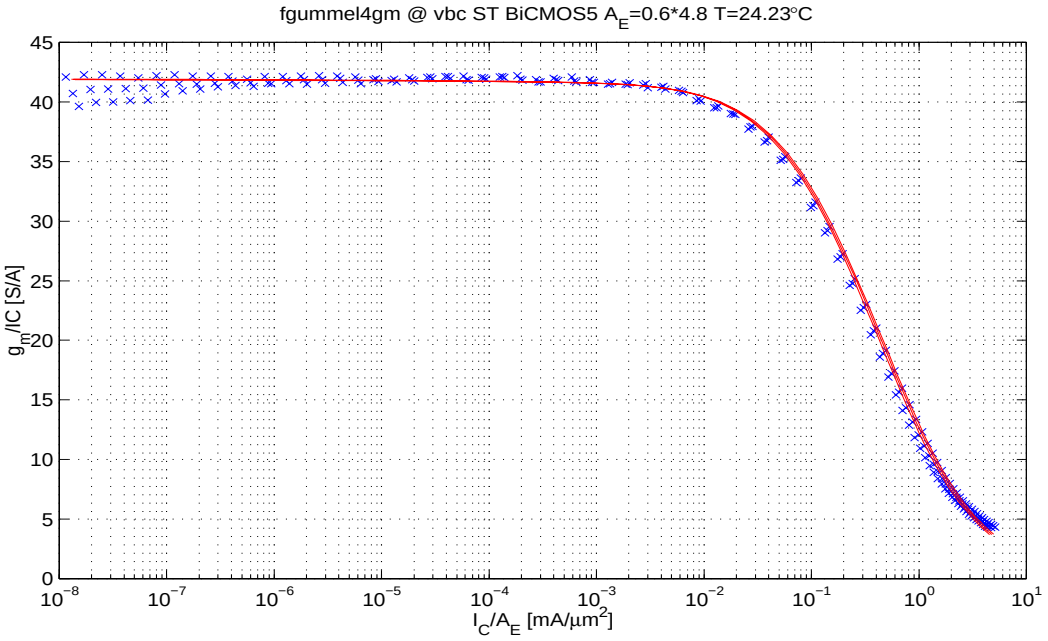

b)

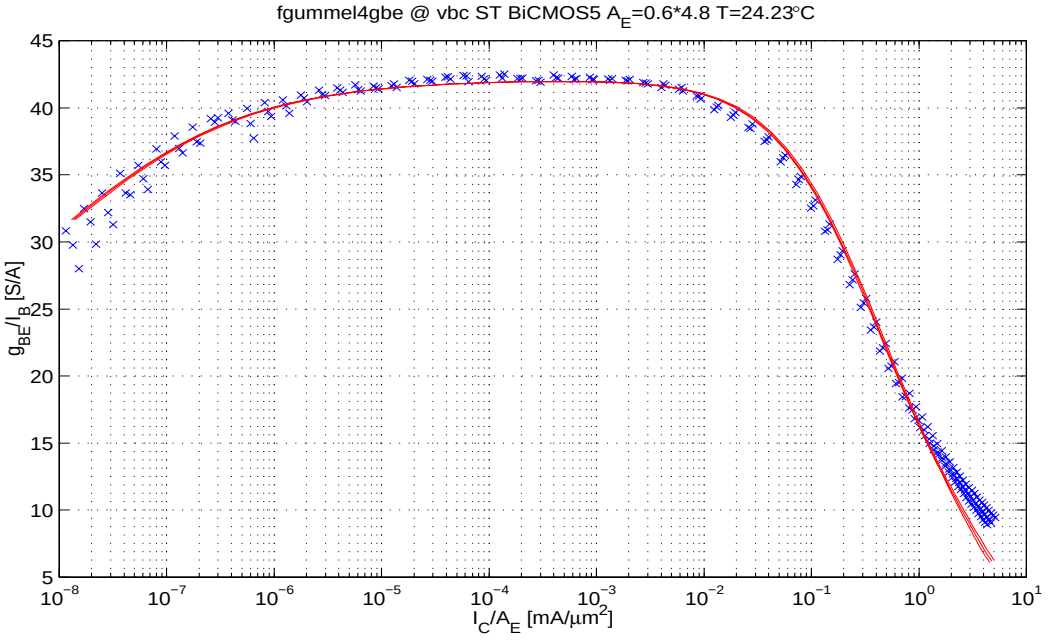

Fig. 1.4/2: Low-frequency transconductance and input conductance vs. collector current density; V_{BC}/V = 0, -1, -2; T=24.2C. Data source: DC measurements.

a)

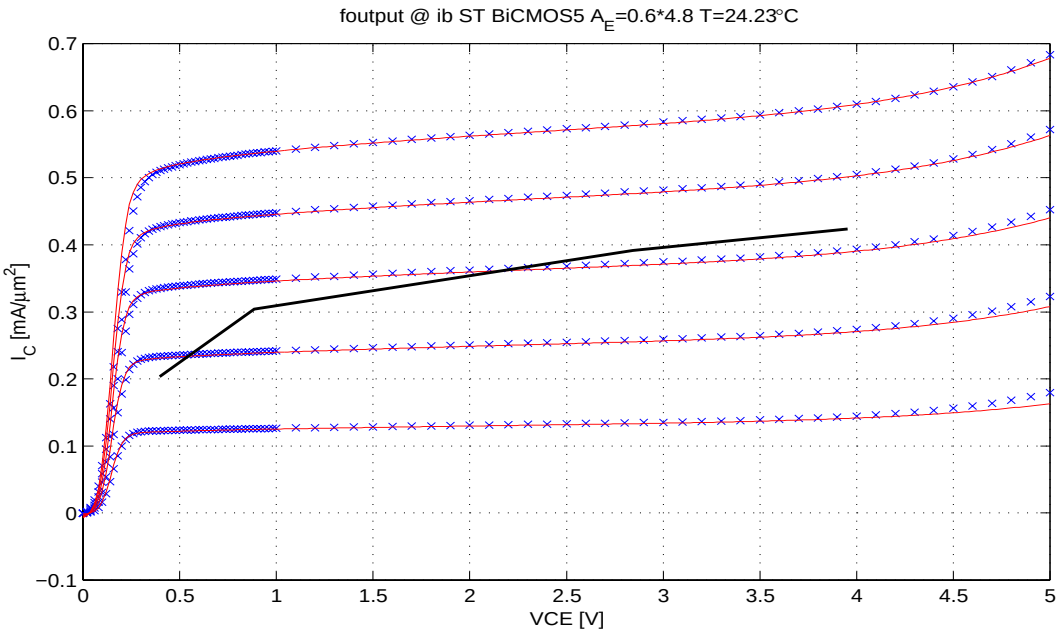

b)

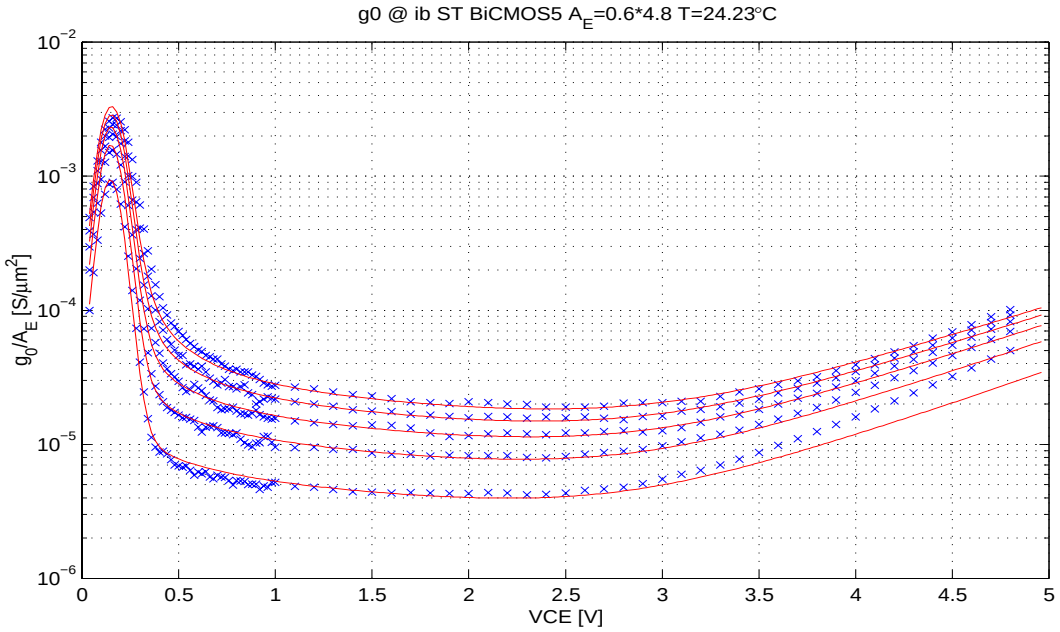

Fig. 1.4/3: Output characteristics and output conductance for $I_B/\mu A$ = 4, 8, 12, 16, 20; T=24.2C.
Data source: DC measurements.
The line indicates the current densities at which f_T peaks.

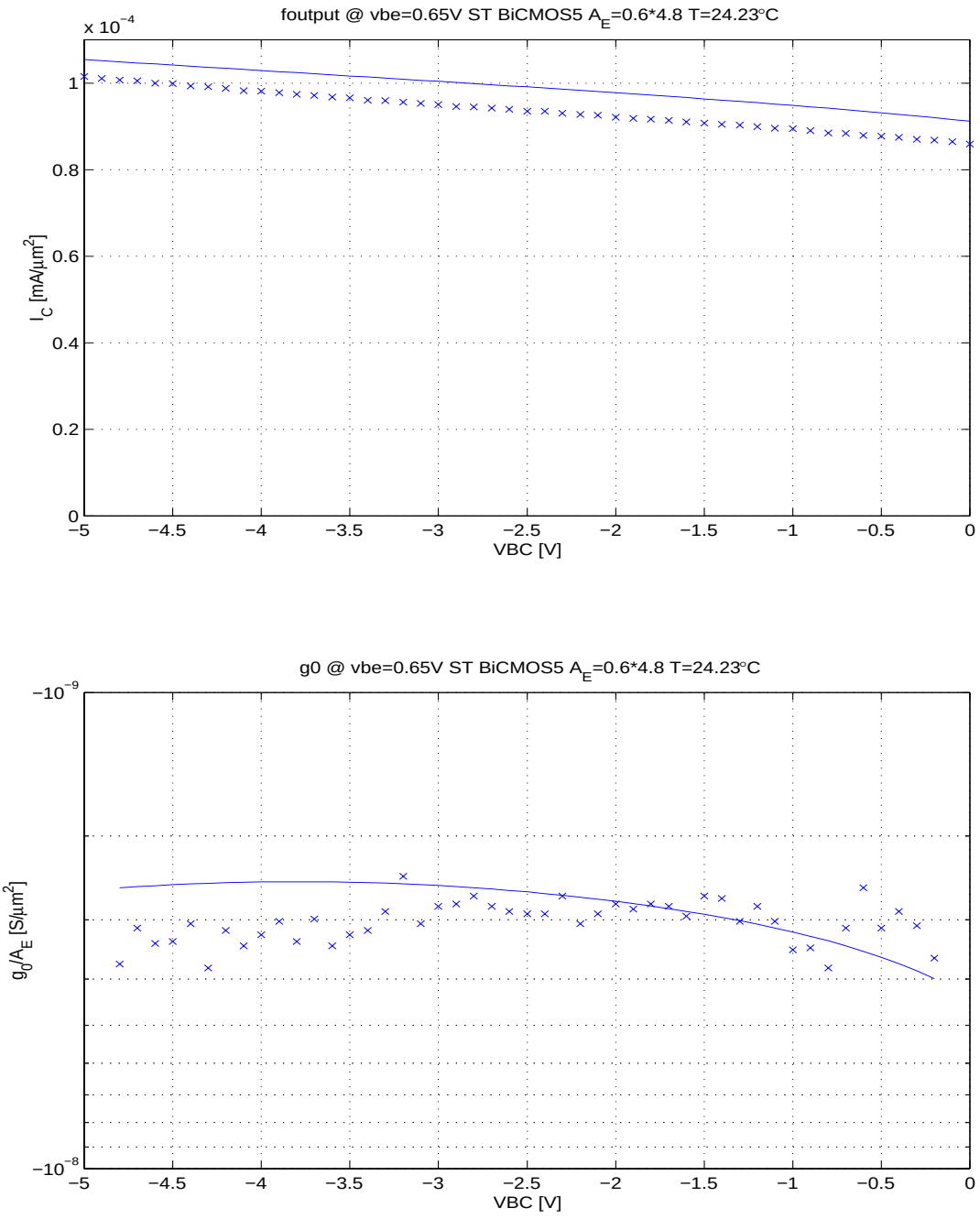

Fig. 1.4/4: Output characteristics and output conductance for V_{BE}/V=0.65; T=24.2C.
Data source: DC measurements.

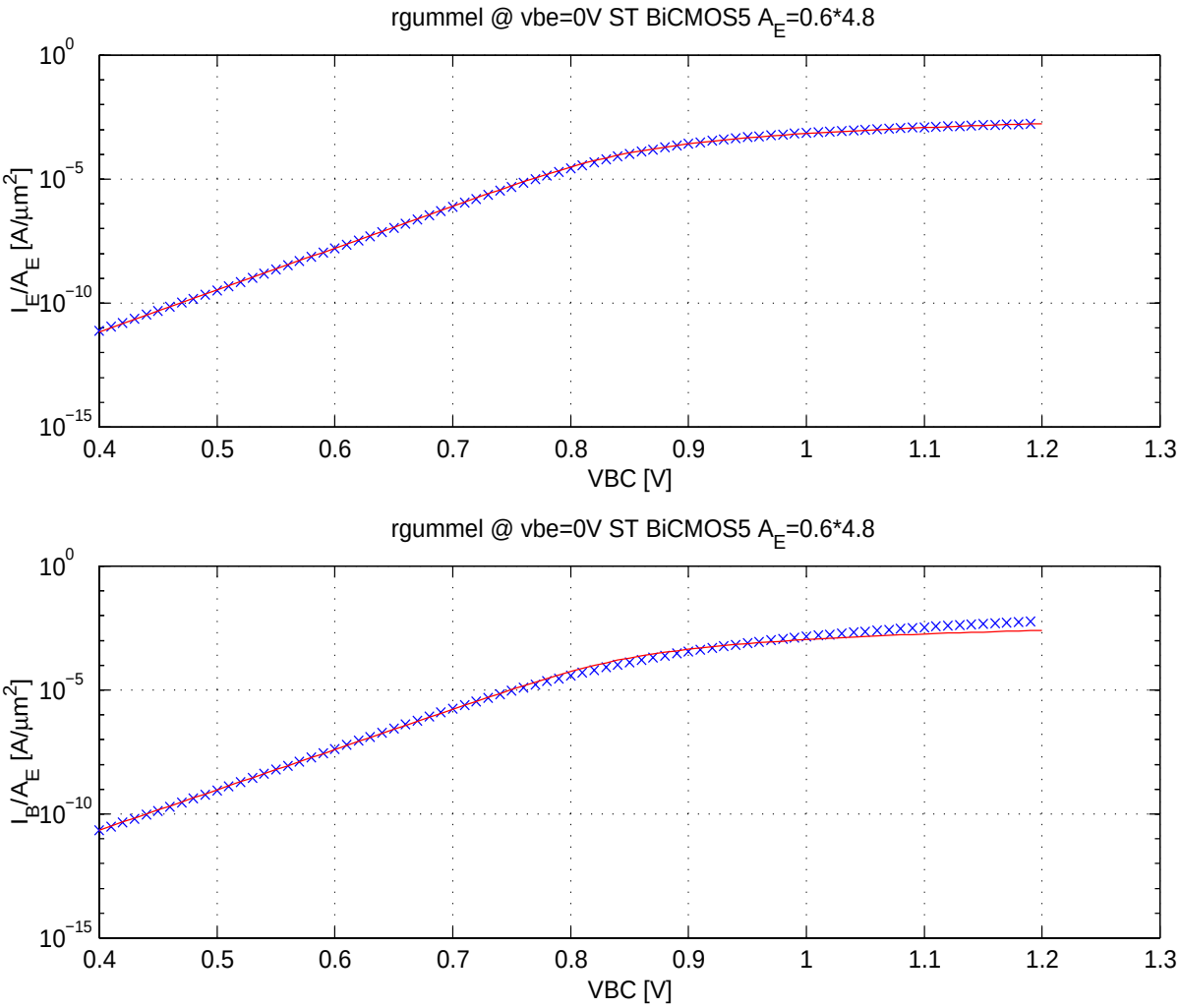

Fig. 1.4/5:Reverse gummel plots for V_{BE}/V=0; T=24.2C.

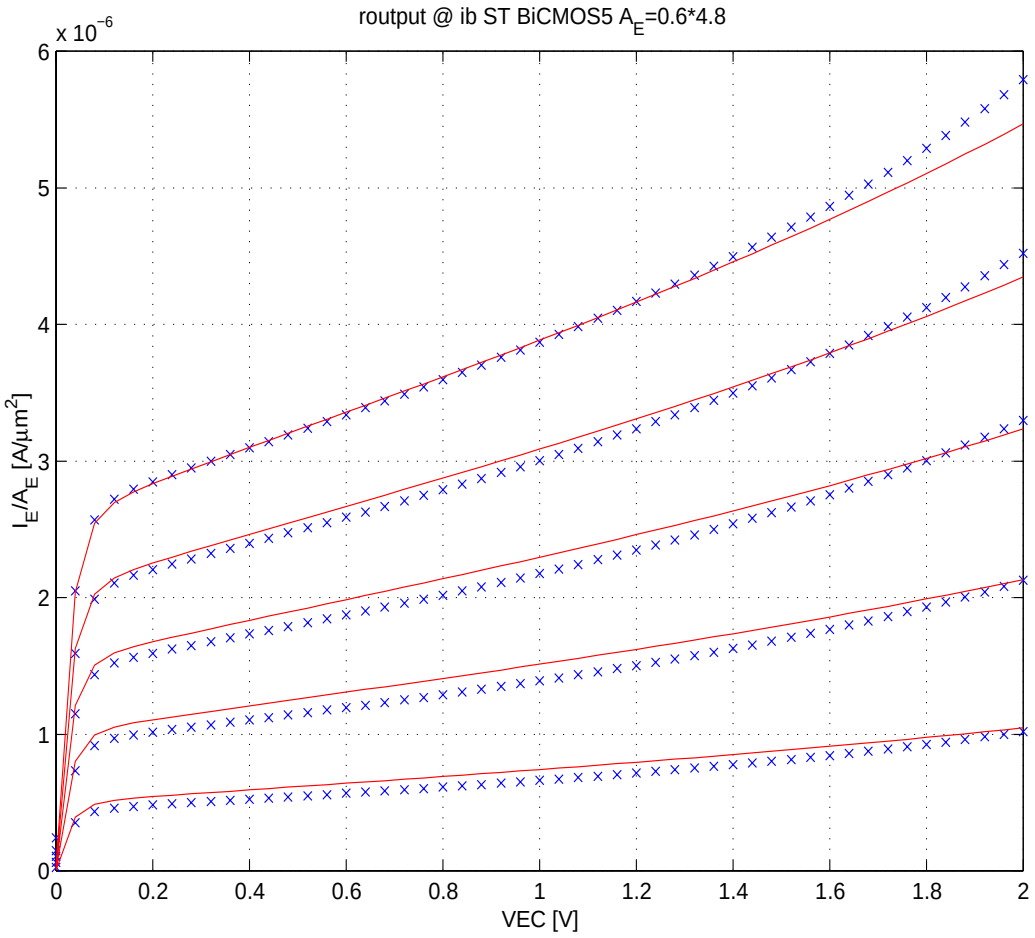

Fig. 1.4/6: Reverse output charactaristics for $I_B/\mu A$=4, 8, 12, 16, 20; T=24.2C
Data source: DC measurements.

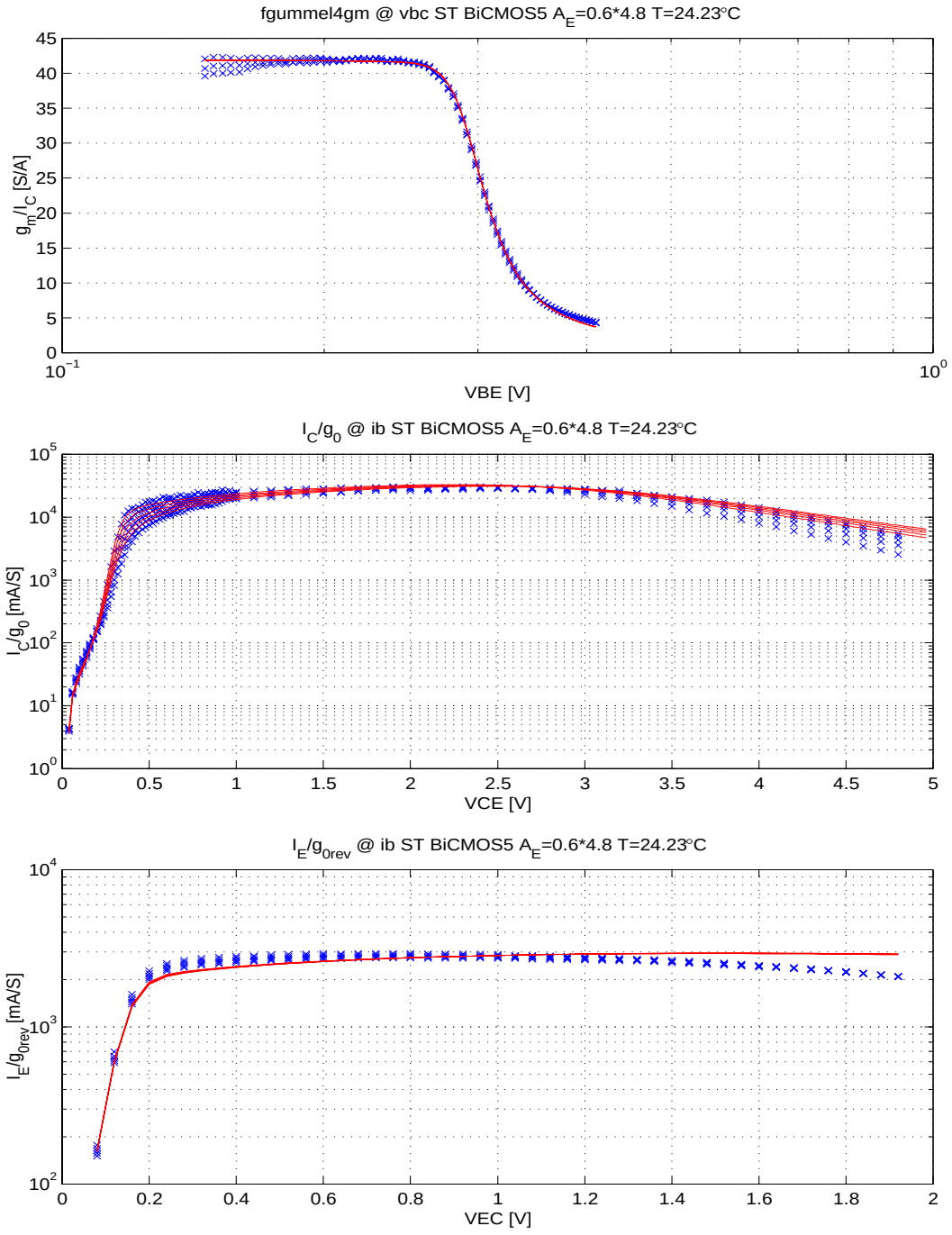

Fig. 1.4/7: Normalized transconductance vs.VBE;
forward and reverse “Early voltage”.

```
‘*’  HICUM / LEVEL2  DC-Satz
‘MODQ’ ‘Tref’ 1
 &HICUM2 c10=4.78E-32     qp0=2.25E-14     ich=5.60E-03     hfc= 0.20
       hfe= 1.00        hjci= 0.68       hjei= 1.00       alit=0.450
       cjei0=8.88E-15   vdei=0.960       zei=0.595        aljei= 2.20
       cjci0=2.12E-15   vdci=0.780       zci=0.474        vptci=1.05E+01
       t0=1.03E-11      dt0h=-1.170E-12  tbvl=5.300E-13   tef0=2.55E-13
       gtfe=  1.00      thcs=3.16E-11    alhc= 8.143      fthc= 0.800
       alqf=0.225
       rci0=3.61E+01    vlim= 0.387      vpt=  4.19       vces= 0.100
       tr=0.00E+00
       ibeis=1.96E-20   mbei=1.0080      ireis=7.00E-17   mrei=2.0000
       ibcis=1E-30      mbci=1.0240
       favl= 03.0       qavl=4E-14
       rbi0= 125.50     fdqr0=0.200      fgeo=0.7570      fqi=1.0000
       fcrbi=0.20
       latb=3.470E+00   latl=0.434
       cjep0=7.95E-15   vdep=0.980       zep=0.437        aljep= 2.30
       ibeps=1.00E-30   mbep=1.0110      ireps=1.00E-30   mrep=2.0000
       ibets=0.00E+00   abet=  0.00
       cjcx0=1.42E-14   vdcx=0.835       zcx=0.452        vptcx=2.30E+00
       ccox=2.78E-15    fbc=0.128
       ibcxs=13E-18     mbcx=1.043
       ceox=1.13E-15    rbx=  31         re= 15.500       rcx= 6
       itss=1.00E-30    msf=1.000        tsf=0.00E+00
       iscs=1.00E-30    msc=1.000
       cjs0=4.01E-14    vds=0.650        zs=0.282         vpts=1.00E+03
       rsu=    0.0      csu=0.00E+00
       kf=0.00E+00      af=1.00E+00
       vgb= 1.160       alb= 1.60E-04    alt0= 0.00E+00   kt0= 0.00E+00
       zetaci=  1.600   alvs=1.00E-03    alces=4.00E-04   zetarbi=  0.830
       zetarbx=  0.180  zetarcx=  0.190  zetare= -0.800
       alfav=8.25E-05   alqav=1.96E-05
       rth=  400.00     cth=0.00E+00  &end
```

Fig. 1.4/8:Set of model parameters for the DC measurement based comparison (DEVICE).